

Magnetic Scattering in the 4f-Intermediate Valence Compound CePd₃

ICNS 2009

Victor Fanelli

Jon Lawrence, CuiHuan Wang

Andrew D. Christianson, Mark D. Lumsden

Eugene A. Goremychkin, Raymond Osborn

Eric D. Bauer, Kenneth J. McClellan

Los Alamos National Laboratory

University of California - Irvine

Oak Ridge National Laboratory

Argonne National Laboratory

Los Alamos National Laboratory

***Work at Los Alamos, supported by NSF, the State of Florida and the US D.O.E.
Work at UC Irvine supported by D.O.E. under Grant No. DEFG03-03ER46036***



UCIRVINE | UNIVERSITY
of CALIFORNIA



UNCLASSIFIED

Slide 1



Introduction



Intermediate valence metals:

- **Fermi Liquid** ground state that evolves towards a high- T **local moment** regime.

The **Anderson lattice model** applicable to these compounds, capturing:

- band-like **coherent character** in the low- T limit, and
- **local moment** character at high- T

Physical properties reveal the effects of the lattice coherence.

However.....

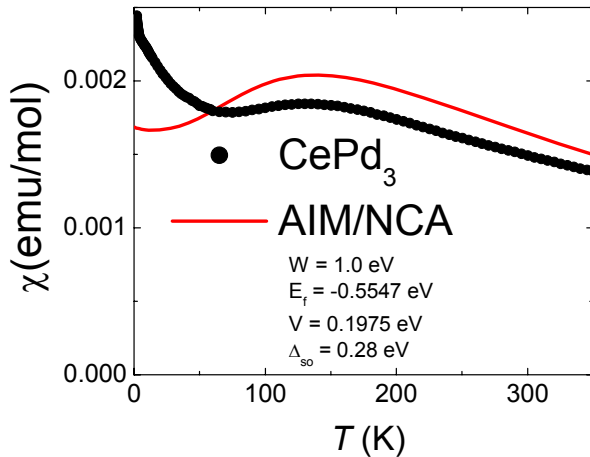
Other properties, depending on spin fluctuations, are better described by the **Anderson impurity model**, despite the magnetic moments sit on a lattice.



Anderson Impurity Model (AIM)



Good semi-quantitative agreement with **AIM**



Pauli Paramagnet :
finite $\chi(T \rightarrow 0)$

Curie-Weiss:
 $\chi(T) = C_J / (T + \theta)$



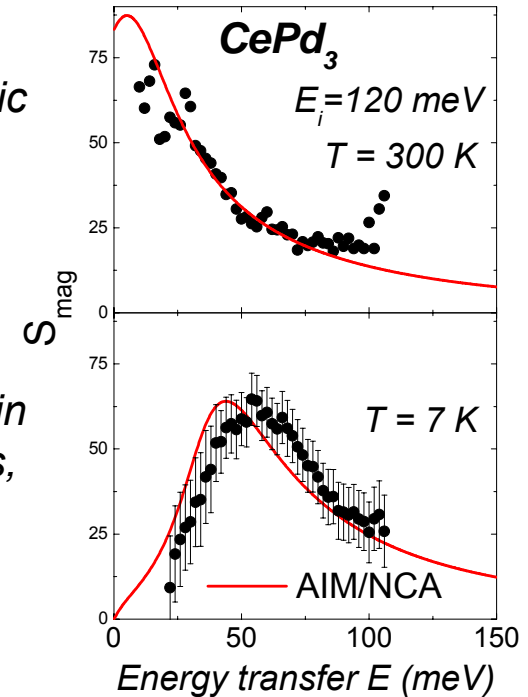
Non-crossing approx. (NCA)

C. Booth, private communication

Quasi-elastic spectrum
 $2\Gamma \sim k_B T_K$



Inelastic spin fluctuations,
 $E_0 \sim k_B T_K$

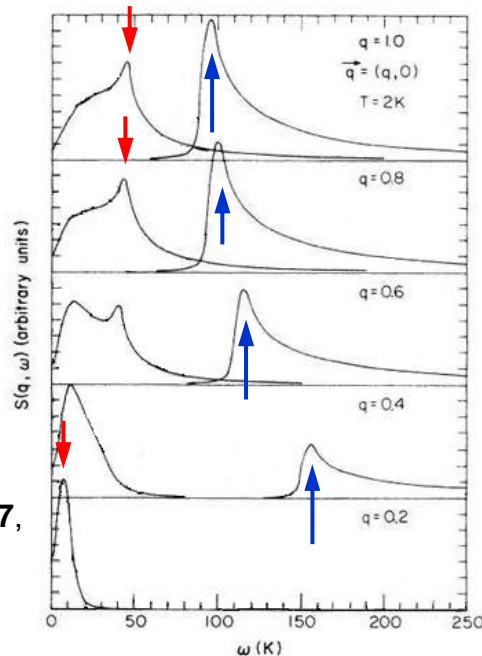




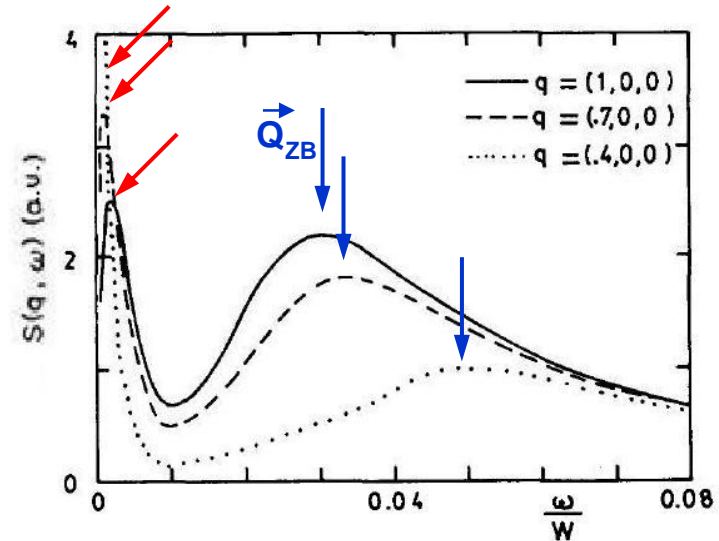
Anderson Lattice Model



Spectrum of $S(Q, E)$ for different values of momentum transfer q



Brandow,
Phys. Rev.B 37,
250 (1988).



Aligia, et al., J. Mag. Mag. Mat. 46, 321 (1985).

- **Inter-band transitions:** The high energy peak is maximum for q at zone boundary. It shifts to high E with decreasing q .
- **Intra-band transitions:** The low energy peak moves to high E as q increases towards zone boundary.



Motivation

magnetic scattering

- *spectral response*
- *dependence over the reciprocal space*

elucidate



*character of the spin
fluctuations:*

Local / coherent ?

*This Q-dependence has
remained an open question*

*Most of INS performed on
polycrystalline samples.*

*Only four compounds studied by INS
on single crystals*

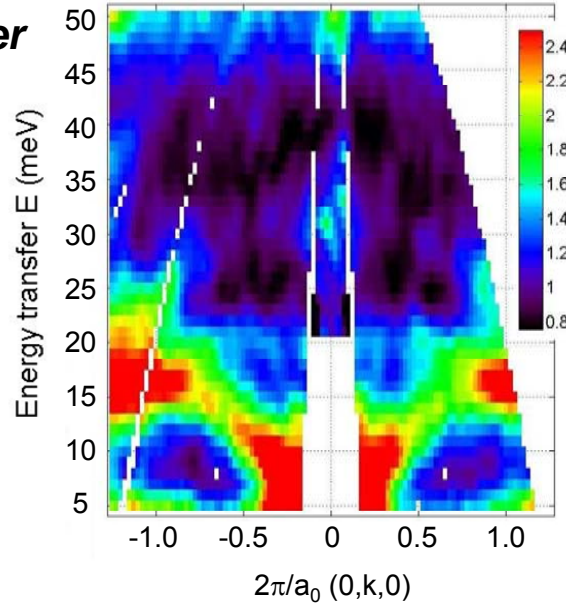


Magnetic and non-magnetic Scattering



MAPS spectrometer

7 K, $E_i=60$ meV



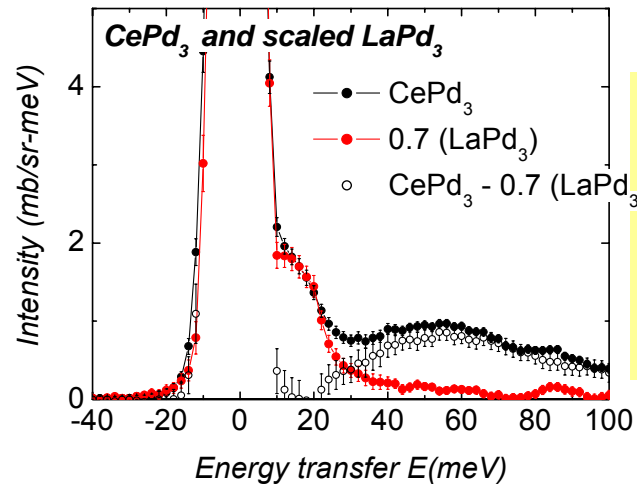
Phonon Scattering dominant

Multiple Scattering (+ Multi-phonons) and Magnetic scattering

Non-magnetic Scattering



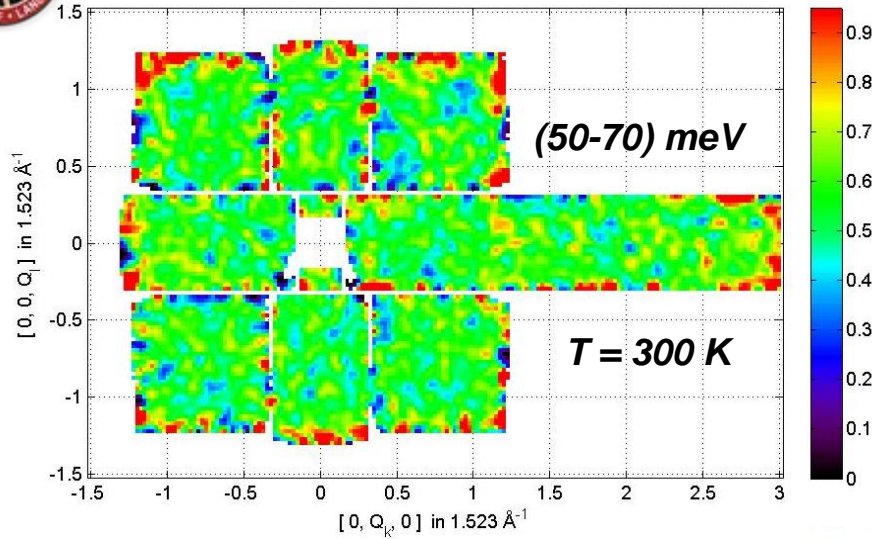
Represented by "scaled LaPd₃"



Difference should account for magnetic contribution to the scattering

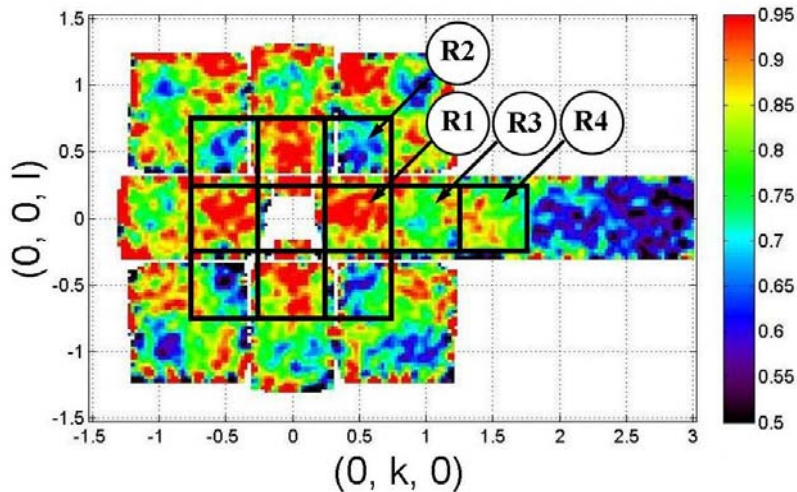


Inelastic Neutron Scattering on $CePd_3$



Distribution of the intensity over momentum transfer space:

- *Relatively uniform at room temperature*



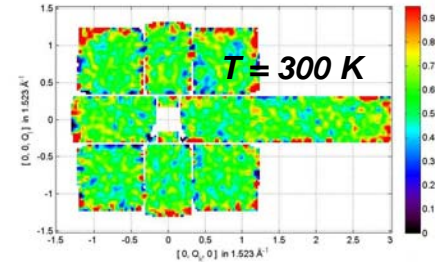
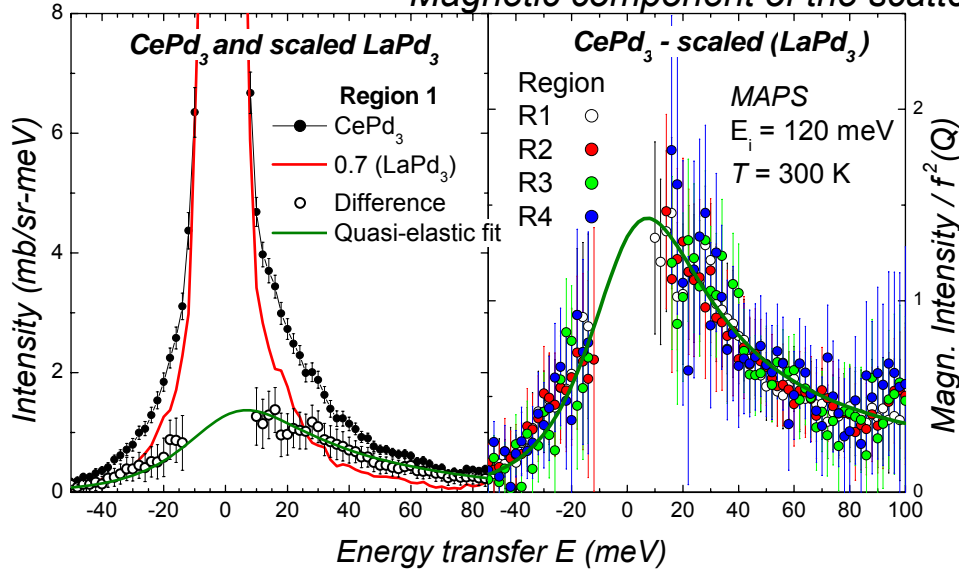
To explore the Q-dependence

Look at different regions in Q-space



CePd₃ at 300 K ($\sim \frac{1}{2} T_K$)

Magnetic component of the scattering



- Quasi-elastic Lorentzian
- Q-independent

$$S_{\text{magn}}(Q, E) = \frac{1}{(1 - e^{-E/k_B T})} f^2(Q) \frac{E A_L}{\pi} \frac{\Gamma}{E^2 + \Gamma^2} \quad \text{with } \Gamma = 27 \text{ meV}$$

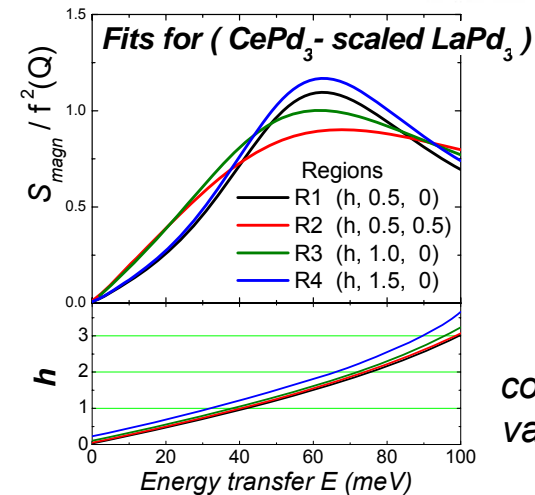
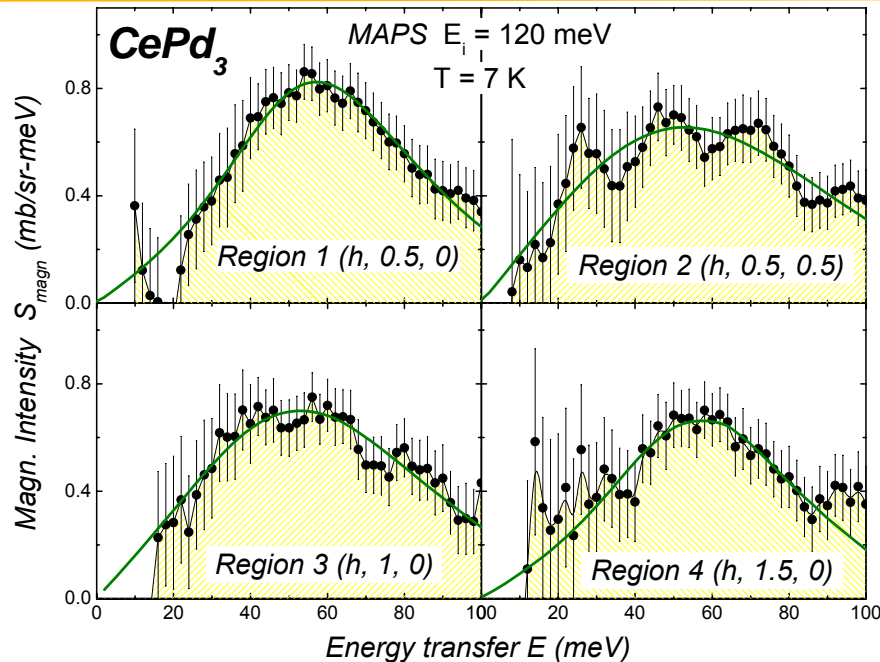
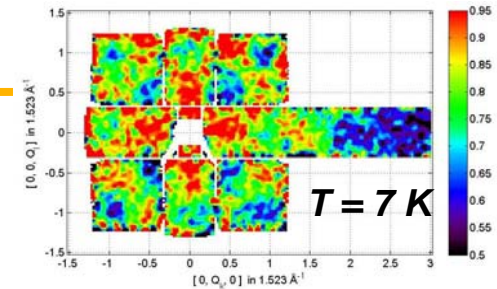
Q-independence implies a **local character** for spin fluctuations as expected for **high-*T* uncorrelated local moment limit**



CePd₃ at 7 K (Low-T regime)



Magnetic scattering of CePd₃ at four regions in the (k,l) plane



In TOF:
component h
varies with E

- Variations of intensity $\sim 25\%$
- Similar Inelastic Lorentzians

Average: $\Gamma = 43.5$ meV
 $E_0 = 45$ meV

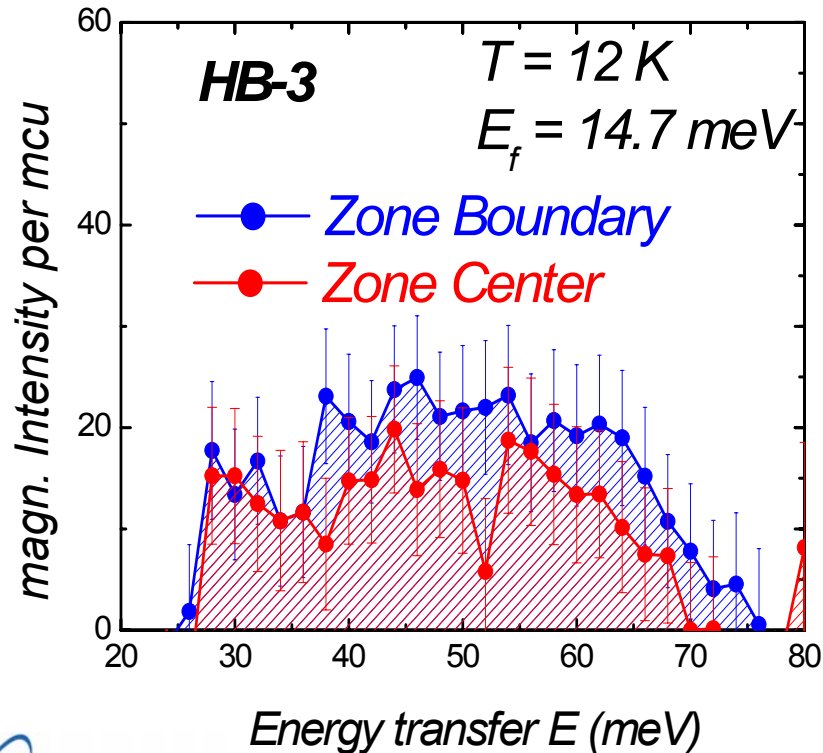
**Q-dependence not as drastic as expected by Anderson Lattice model
(NO shift of spectral weight)**



CePd₃ (Low-T) Triple-axis spectrometer

Constant-Q scans:

- at the Brillouin **zone boundary** (2.5, 1.5, 0)
- at the Brillouin **zone center** (2, 2, 0)



Again:

Difference between **ZB** and **ZC** is **NOT** at all as the pronounced variation predicted by the ALM



Discussion / Conclusions



Conclusions (i)

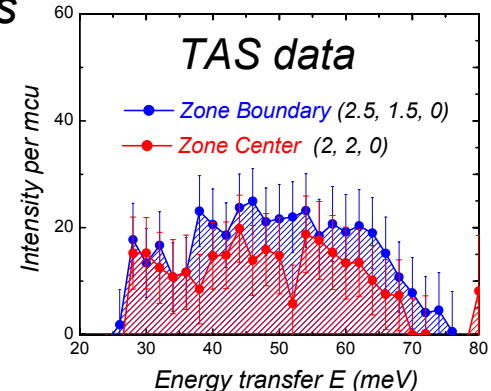
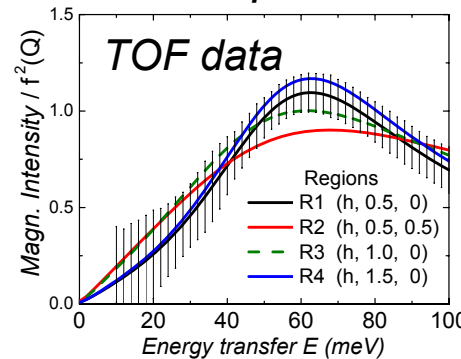
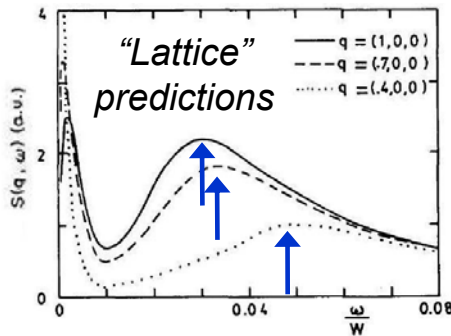


1) High-temperature magnetic scattering:

**Q-independent, quasi-elastic spectrum
proving
Local character of uncorrelated magnetic moments**

2) Low-temperature magnetic scattering:

- Broad Inelastic Lorentzian + weak Q-dependence
- **Qualitatively different from ALM predictions**



Much more like the predictions of the AIM

Similar “Kondo-like” spectral response: $\left\{ \begin{array}{l} \text{YbAl}_3, (\text{Christianson, PRL, 2006}) \text{ YbInCu}_4 (\text{Lawrence, PRB 1997}), \\ \text{CeInSn}_2, (\text{Murani, PRL 2008}) \end{array} \right.$

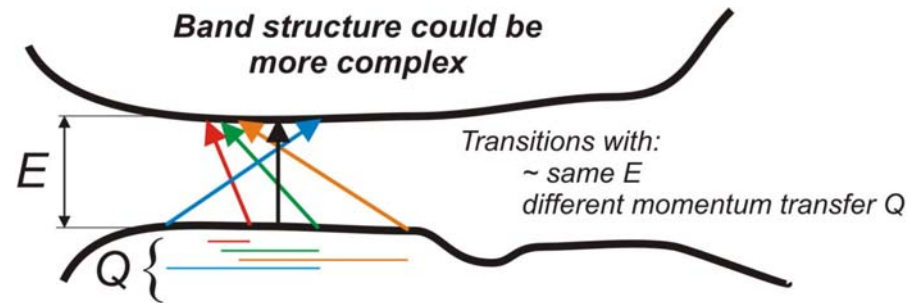


Conclusions (ii)

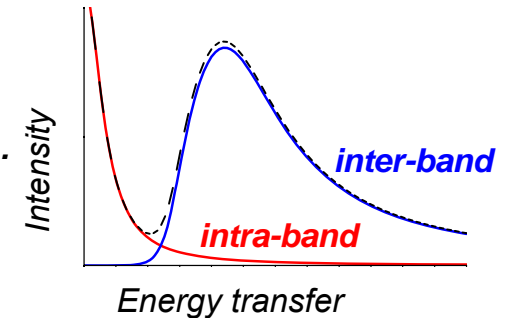


Possible reasons for the failure of ALM predictions for spin dynamics of IV comp.

a) **Band structure more complex**
than just two hybridized bands.
These bands remain to be calculated.



b) There may be significant **overlap** of the **intra-band** Fermi Liquid excitations with the **inter-band** transitions.
We are uncertain about the energy scale of the former (above 10 meV?)



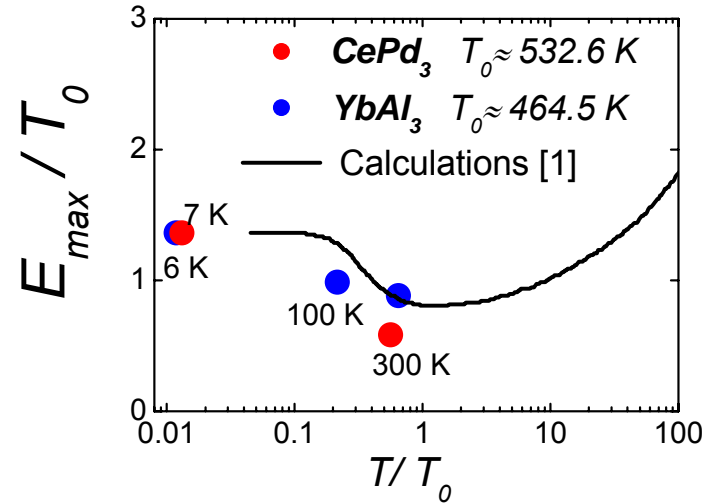
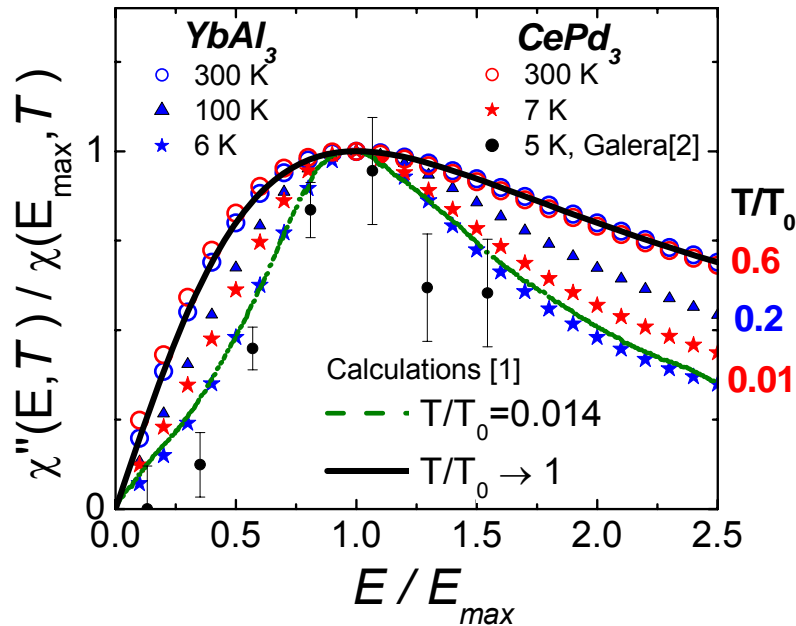
c) ALM approximations may require improvements. Some are versions of mean field (MF) approx. which do not necessarily get the **excitation energies away from the ϵ_F** correctly.



Conclusions (iii)



3) Evolution with temperature: Agreement with AIM calculations



[1] Cox, Bickers, Wilkins, J. Appl. Phys. **57**, 1 (1985)

[2] Galera, et al., J. Magn. Magn. Mat. **47-48**, 139 (1985).

*Excitations in the Anderson lattice are much more like those of an Anderson **impurity** than has been previously recognized*



Thank you!



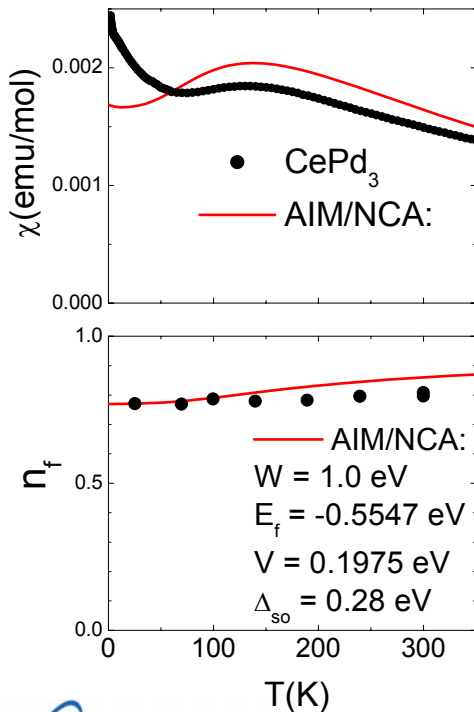
Supporting Slides



Anderson Impurity Model (AIM)



Even though RE's ions sit on a **lattice**, good semi-quantitative agreement with **AIM**



Curie-Weiss:
 $\chi = C_J / (T + \theta)$



Pauli Paramagnet :
finite $\chi(0)$

Integral valence ($n_f \rightarrow 1$)

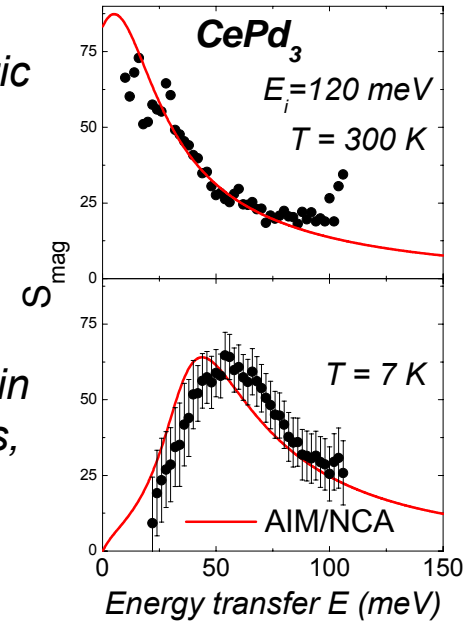


Non-integral valence

Quasi-elastic spectrum
 $2\Gamma \sim k_B T_K$



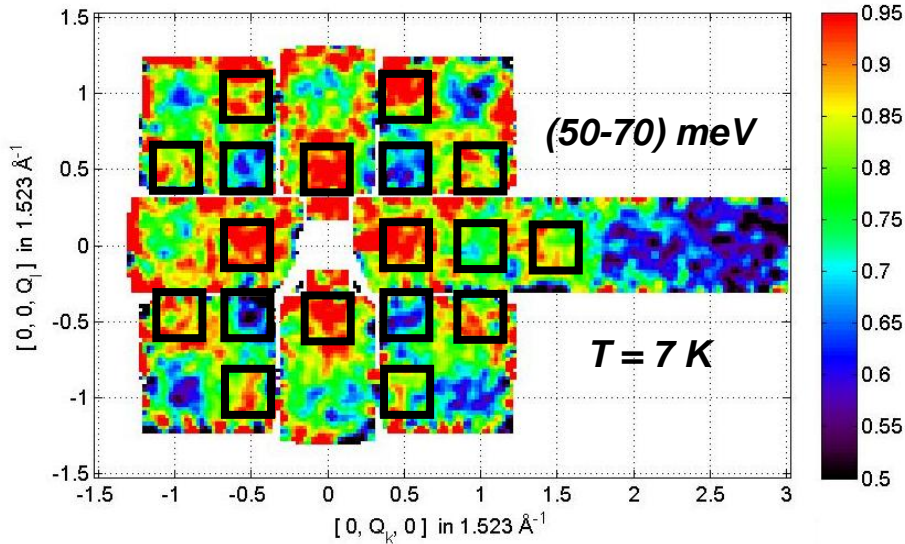
Inelastic spin fluctuations,
 $E_0 \sim k_B T_K$



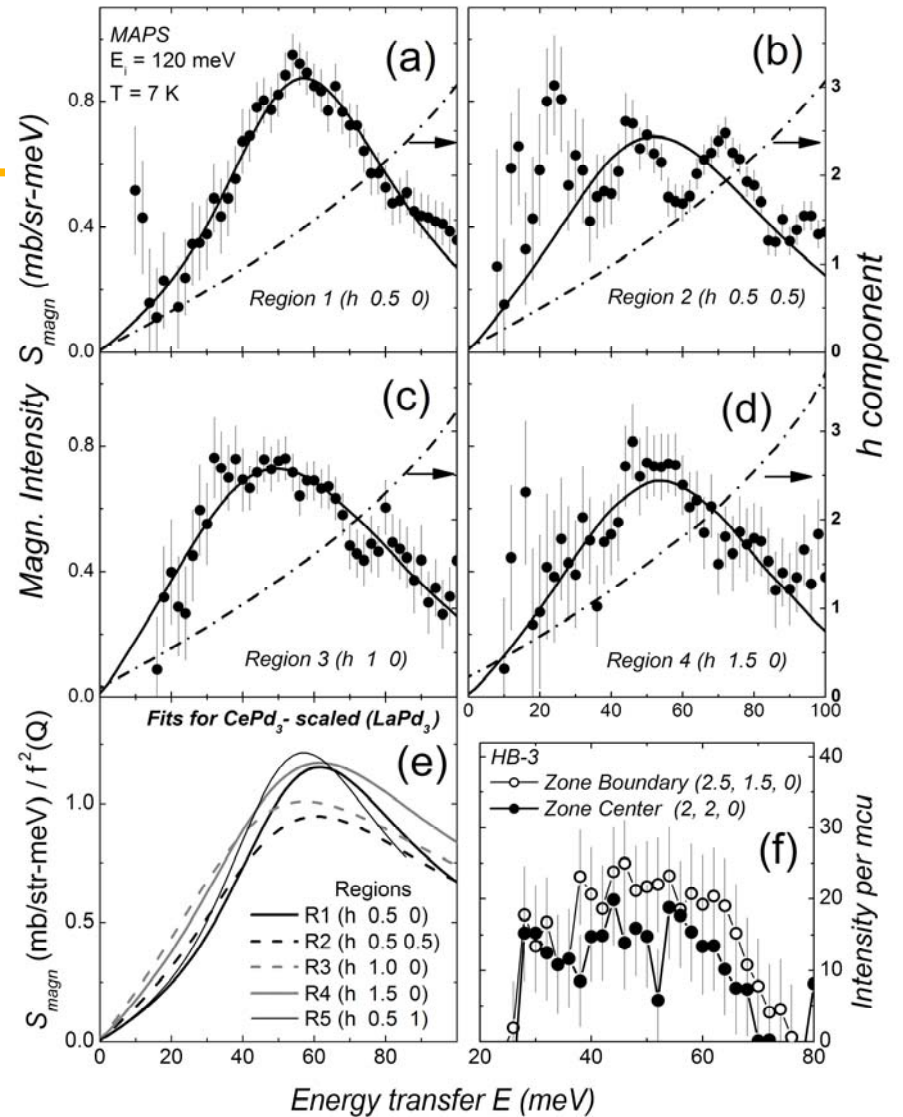
Non-crossing approx. (NCA)

C. Booth, private communication

Smaller Q-Regions



Q-region	T (K)	E_0 (meV)	Γ (meV)
Region 1	7	52.6 ± 0.8	32 ± 1
Region 2	7	42 ± 5	41 ± 5
Region 3	7	37 ± 3	44 ± 4
Region 4	7	46 ± 2	41 ± 4
average	7	46 ± 3	39.5 ± 4
all regions	300	0	23.3 ± 0.8





Conclusions (i)



1) High-temperature magnetic scattering:

*Q-independent quasi-elastic Lorentzian spectrum
proving*

*Local character of spin fluctuations for
uncorrelated magnetic moments*

2) Low-temperature magnetic scattering:

(inelastic Lorentzian + weak Q-dependence)

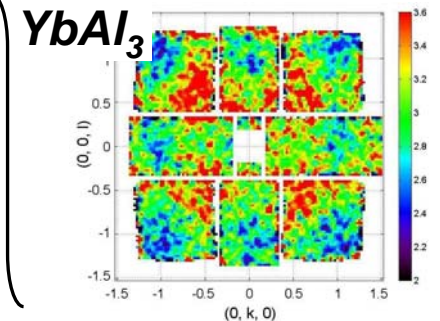
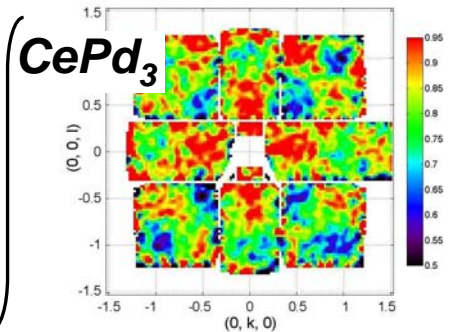
Much more like the predictions of the AIM than the ALM.

Similar “Kondo-like” spectral response:

$YbAl_3$, Christianson, et al, Phys. Lett. 96, 117206 (2006)

$YbInCu_4$, Lawrence, et al, Phys. Rev. B 55, 14467 (1997)

$CeInSn_2$, Murani, et al, Phys. Rev. Lett. 101, 206405 (2008)



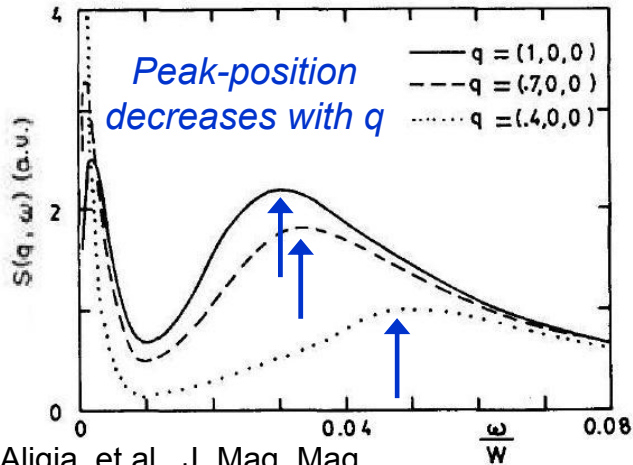


Conclusions (iii)



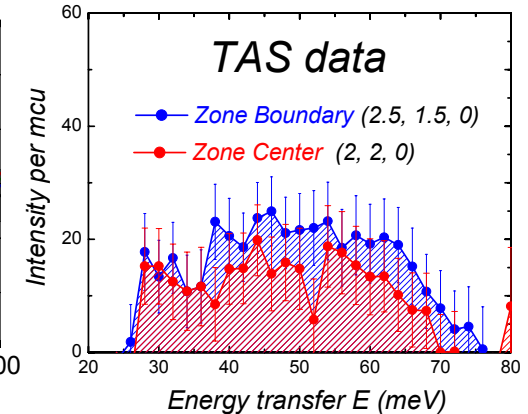
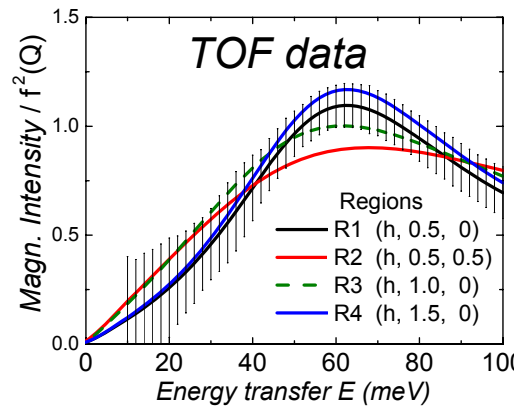
3) Low-T magnetic scattering qualitatively different from ALM predictions

“Lattice” predictions



Aligia, et al., J. Mag. Mag. Mat. **46**, 321 (1985).

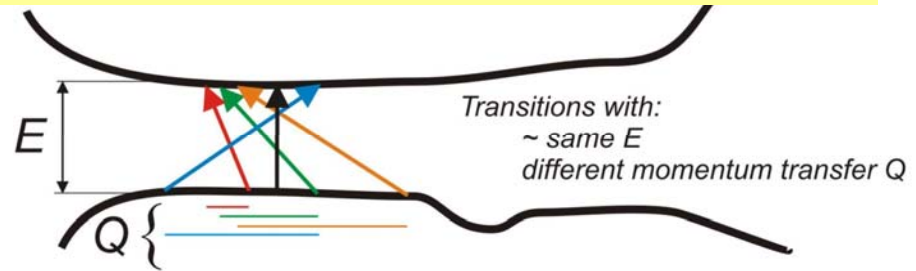
CePd₃ at low-T, for different Q's



- **Q-dependence** not at all as severe as ALM prediction
- **No gap** in the scattering

Band structure more complex than just two hybridized bands.

These bands remain to be calculated.



Values for CePd₃ using big Q-regions

Q-region	T (K)	E_0 (meV)	Γ (meV)	χ_{DC} (10^{-3} emu/mol)
Average value	8	45 ± 2	43.5 ± 4	1.93 ± 0.2
All zones	300	0	26.6 ± 0.7	1.98 ± 0.03

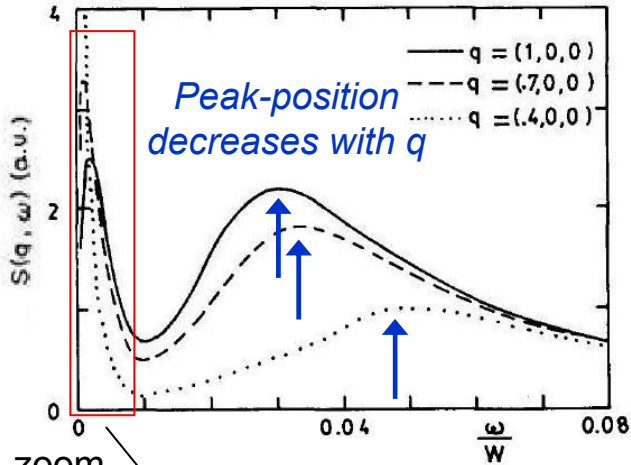


Conclusions (iii)

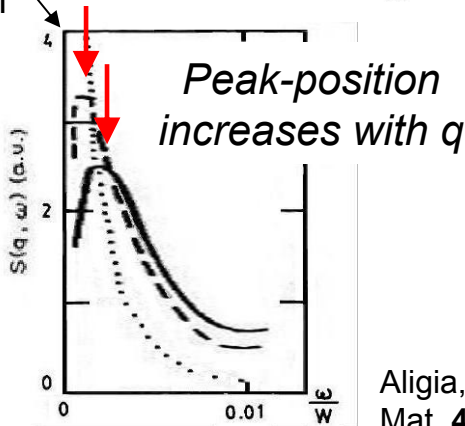


Low-T magnetic scattering differs from the predictions of the ALM.

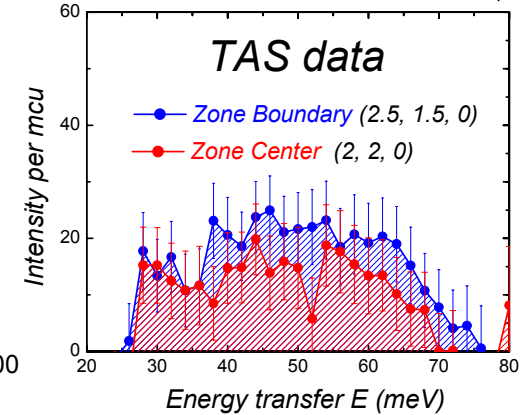
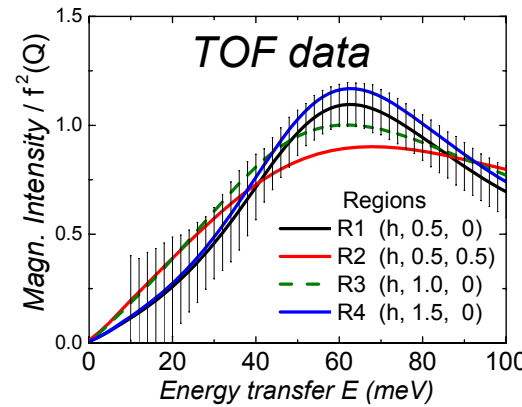
“Lattice” predictions
 $S(Q,E)$ for different Q 's



zoom



Magnetic Intensity spectra:
 $CePd_3$ at low-T, for different Q 's



- **Q-dependence** not at all as severe as ALM prediction
- **No gap** in the scattering
(Overlap of intra- and inter-band transitions?)

Aligia, et al., J. Mag. Mag. Mat. **46**, 321 (1985).



Anderson Lattice Model (ALM)

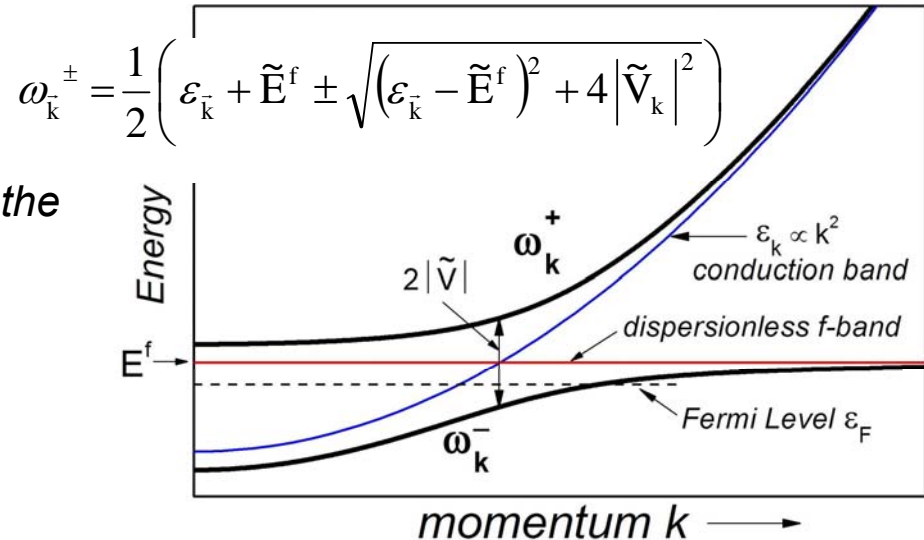


$$\mathbf{H} = \sum_{\vec{k}, \sigma} \varepsilon_{\vec{k}} C_{\vec{k}, \sigma}^{\dagger} C_{\vec{k}, \sigma} + \sum_i \left[\sum_{\sigma} E^f f_{i, \sigma}^{\dagger} f_{i, \sigma} + \sum_{\vec{k}, \sigma} \left(v_{\vec{k}} f_{i, \sigma}^{\dagger} C_{\vec{k}, \sigma} + v_{\vec{k}}^* C_{\vec{k}, \sigma}^{\dagger} f_{i, \sigma} \right) + U f_{i, \uparrow}^{\dagger} f_{i, \uparrow} f_{i, \downarrow}^{\dagger} f_{i, \downarrow} \right]$$

Dispersion of the hybridized bands.

The direct gap has a value $2\tilde{V}$

Coulomb interaction U renormalizes the parameters V and E^f .



Basic Phenomenological Description

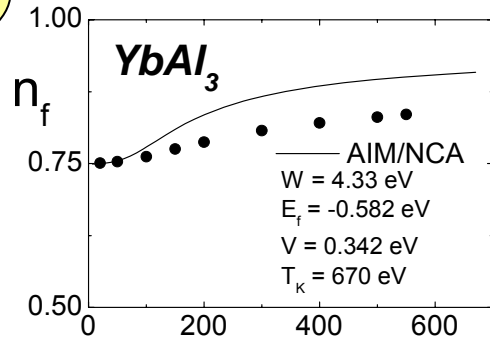
**Low-T
FERMI LIQUID**

- Non-integral valence ($n_f < 1$)

- Pauli Paramagnet
finite $\chi(0) \sim \mu_B^2 N(\epsilon_F)$

- Linear Specific Heat
 $C(T) \sim \gamma T$
 $\gamma = 1/3 \pi^2 N(\epsilon_F) k_B^2$

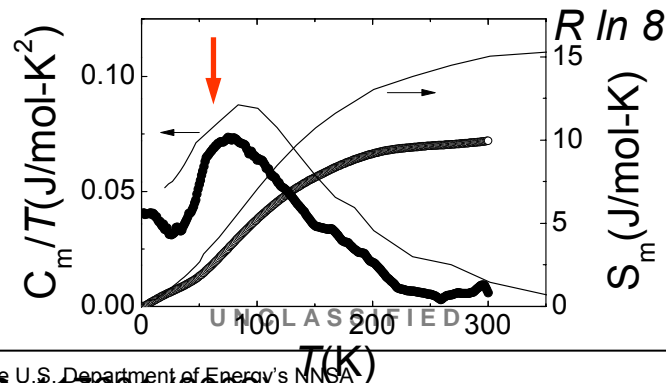
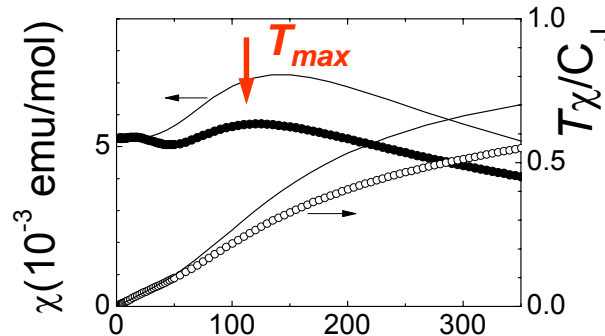
crossover to



**High -T
LOCAL MOMENT
PARAMAGN**

- Integral valence ($n_f \rightarrow 1$)

- Curie-Weiss: $\chi = C_J / (T + \theta)$

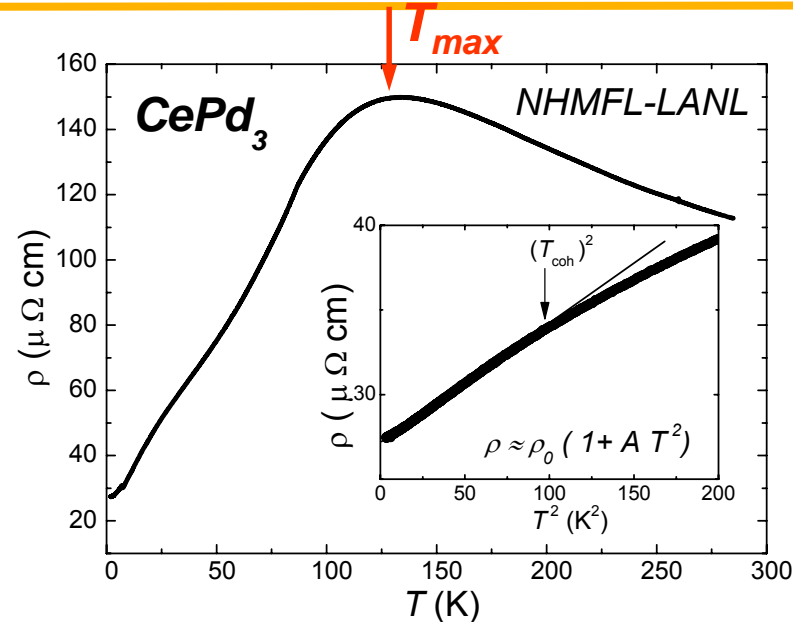


- Entropy: $S_m \rightarrow R \ln(2J+1)$

- Onset of **coherence**

i) Bloch's law

ii) $\rho \propto T^2$



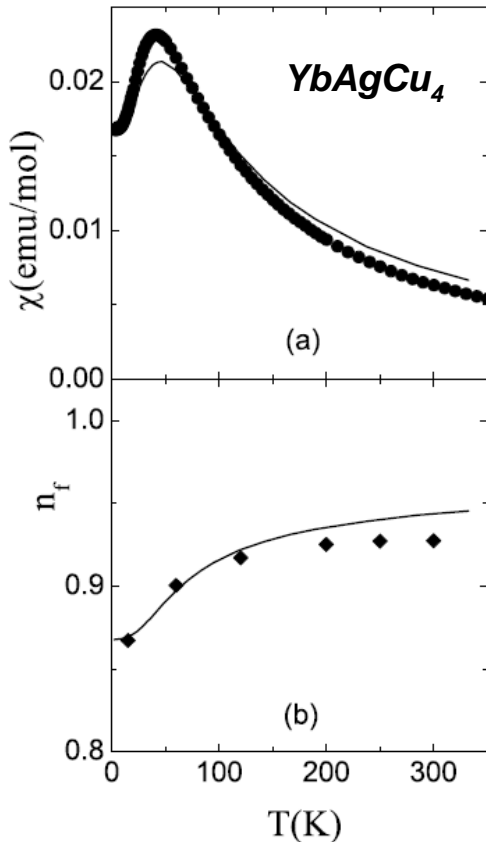
- Scaling**

$$1/\chi_0, 1/\gamma, \Gamma, E_0 \propto k_B T_{\text{max}}$$

Thermodynamic properties are universal function of a scaled temperature T_{max}

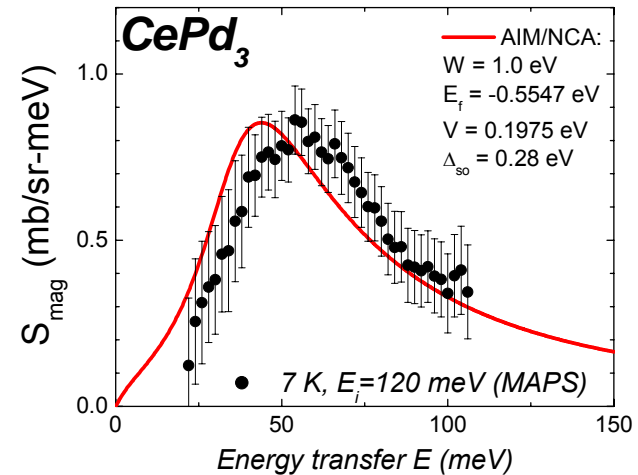
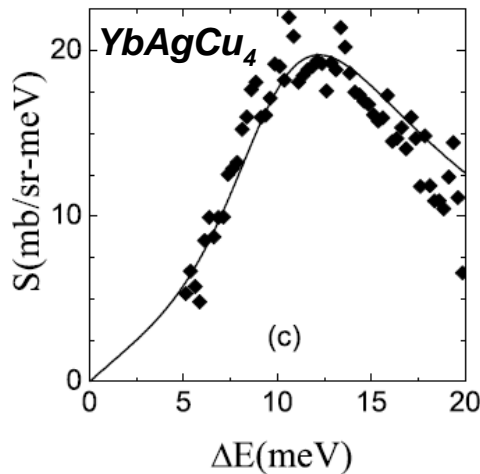
Even though RE's sit on a lattice, and are not "impurities", good agreement with **AIM**

- **Qualitative agreement**
- **Some quantitative agreement**
- **Slower crossover than AIM prediction**



Non-crossing approx.
(NCA)

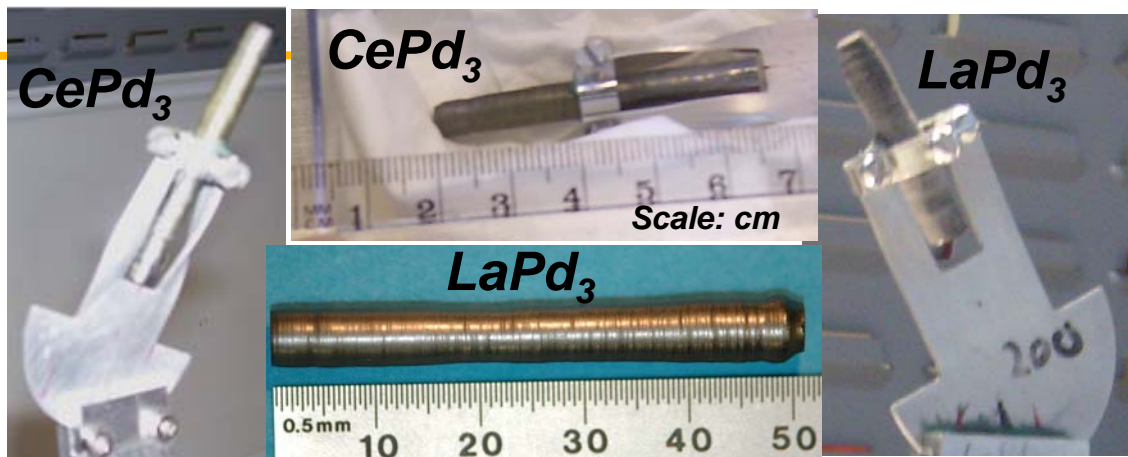
Lawrence et al, Phys. Rev. B
63, 054427 (2001).



Calculation: C. Booth,
private communication

$CePd_3$ (18 g) $LaPd_3$ (11 g)
Grown by Czochralski method
Annealed at $950^\circ C$ (6 days)

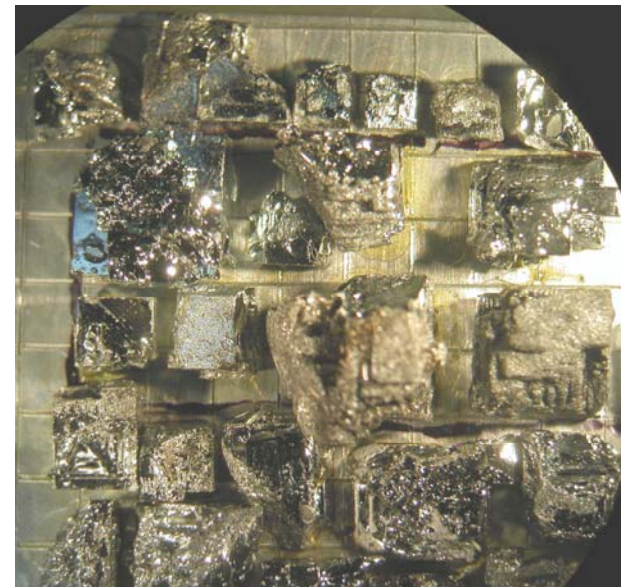
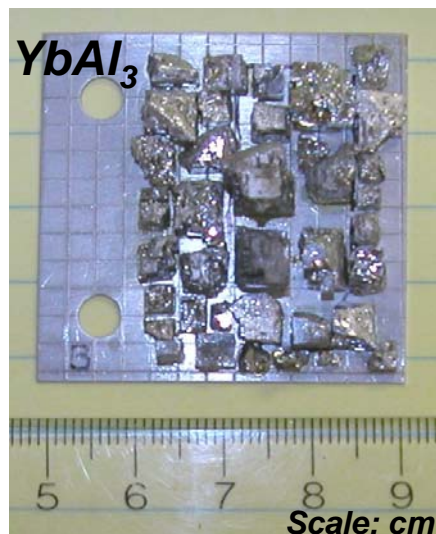
E. D. Bauer,
C. H. Wang,
K. J. McClellan



$YbAl_3$ (≈ 5 g)*
Grown by self-flux method

A. D. Christianson,
E. D. Bauer

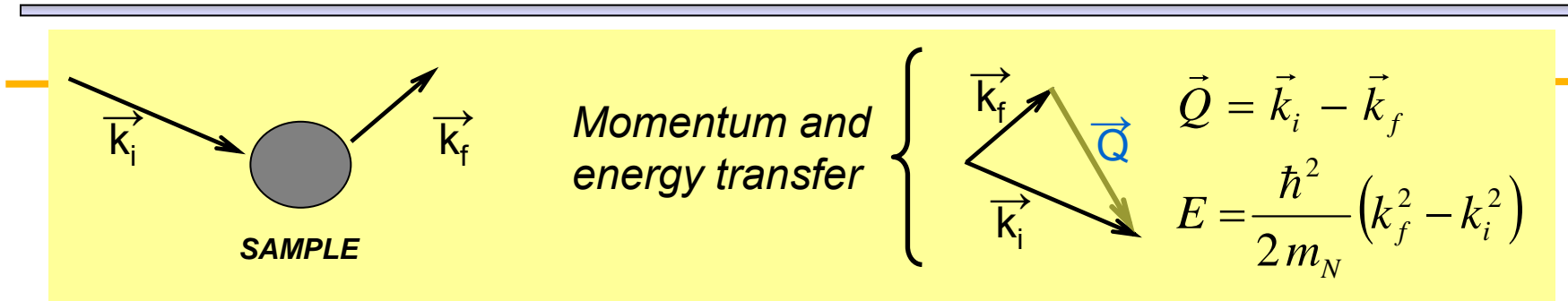
* In the pictures: **not** the actual set-up used in the experiments reported in this work



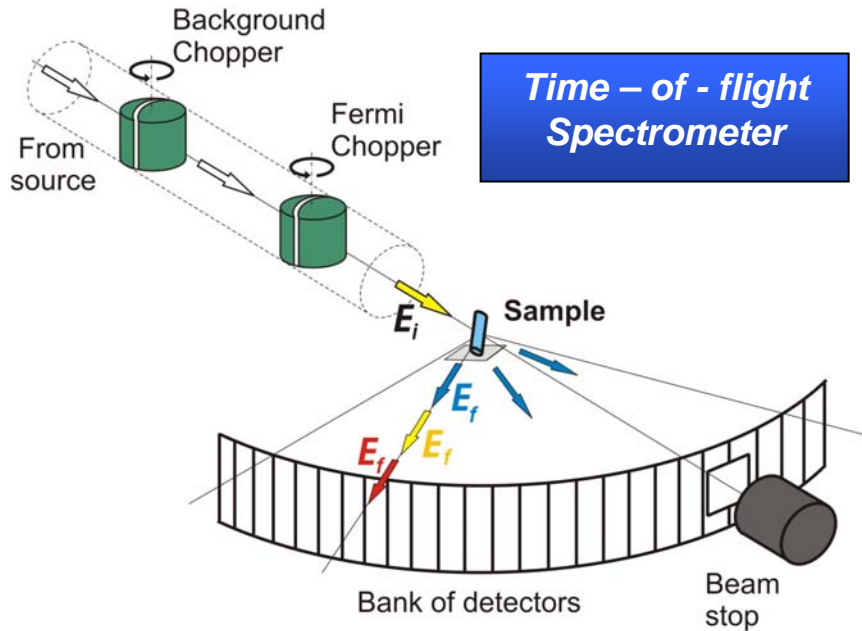
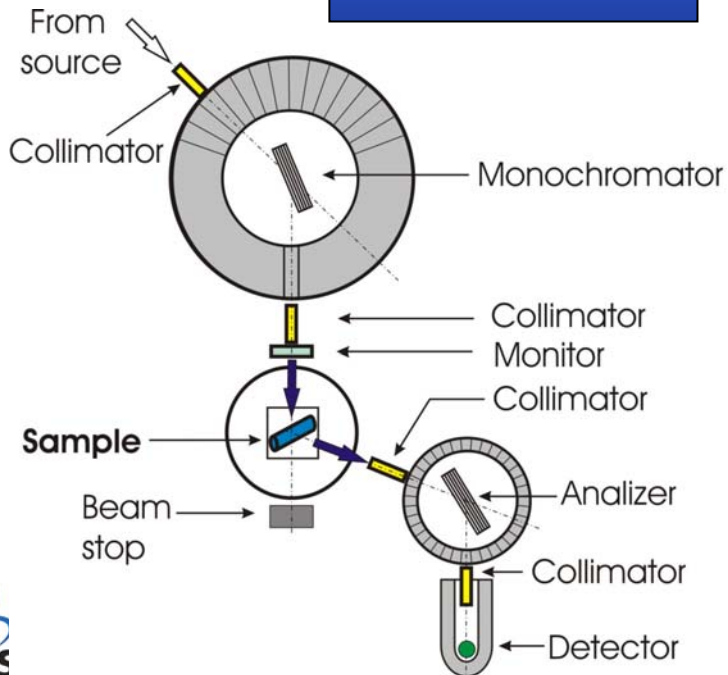
UNCLASSIFIED

Slide 27

Inelastic Neutron Scattering



Triple - axis Spectrometer



Time - of - flight Spectrometer

Scattering cross section σ $\frac{d^2 \sigma}{d\Omega dE} = \frac{k_f}{k_i} \underbrace{S(\vec{Q}, E)}_{\text{Scattering Function}}$

Case of Magnetic Scattering

$$S_{\text{mag}}(\vec{Q}, E)$$

S_{mag} : \approx **Fourier Transform of the moment-moment correlation function.**

S_{mag} **Related to the imaginary part of the dynamic susceptibility χ**

$$S_{\text{mag}}(\vec{Q}, E) = \frac{1}{\pi} \left[\frac{1}{1 - e^{-E/k_B T}} \right] \chi''(\vec{Q}, E)$$

$$\chi''(Q, E) \propto \underbrace{f^2(Q)}_{\text{Magnetic form factor}} \frac{E \chi_{\text{DC}} \Gamma_Q}{2\pi} \underbrace{\left(\frac{1}{(E - E_{0,Q})^2 + \Gamma_Q^2} + \frac{1}{(E + E_{0,Q})^2 + \Gamma_Q^2} \right)}_{\text{Power-spectrum}}$$

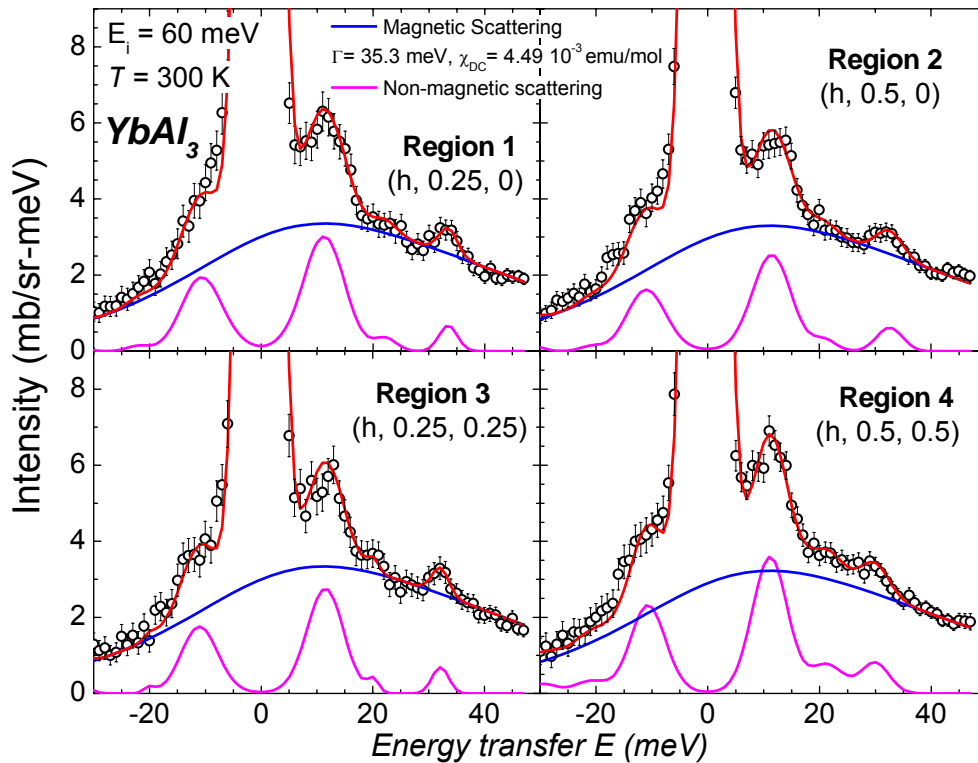
Magnetic form factor

Power-spectrum

Inelastic Neutron Scattering on $YbAl_3$

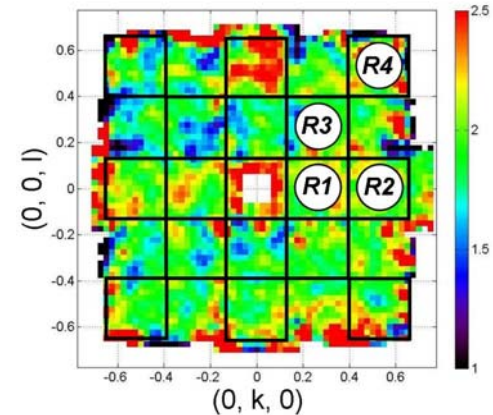
*Measurements at 300 K, 100 K and 8 K
on time – of – flight spectrometer
(no non-magnetic analog compound)*

YbAl₃ Magnetic scattering at 300 K



We have not measured INS on a non-magnetic counterpart compound

Regions in Q-space



Intensity = (Magn. Comp.) + (Non-magn. Comp)

Assuming: (Non-magn) = 3 Gaussian peaks + elastic peak

Q-indep, Quasi-elastic Lorentzian

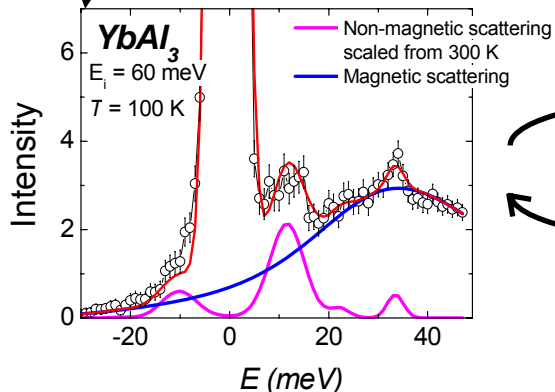
Γ = 35 meV

YbAl₃ magnetic scattering

300 K

$E_i = 60 \text{ meV}$

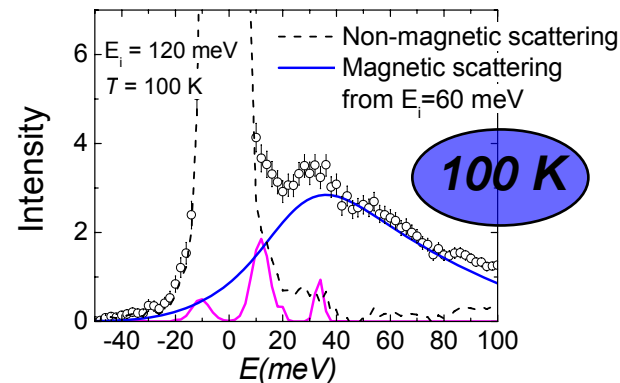
Temp-scale
3-Gaussian



Check
use Lorentzian

If good agreement

$E_i = 120 \text{ meV}$



100 K

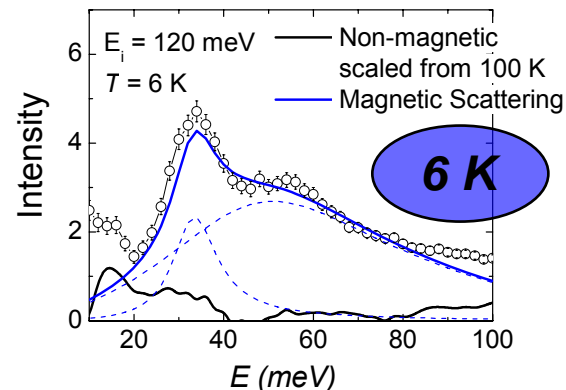
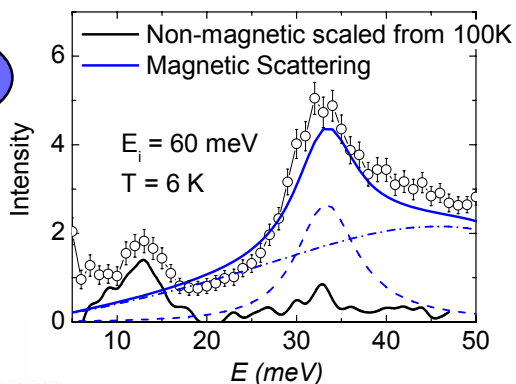
100 K

$$(Magn.) = I - (Non-magn)$$

$$I = (Magn) + (Non-magn)$$

6 K

Temp-scale
Non-magnetic



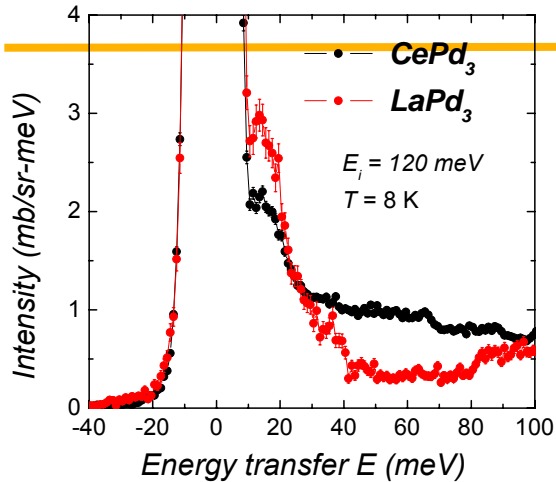
6 K

$$(Magn.) = I - (Non-magn)$$

$$(Magn.) = I - (Non-magn)$$

UNCLASSIFIED

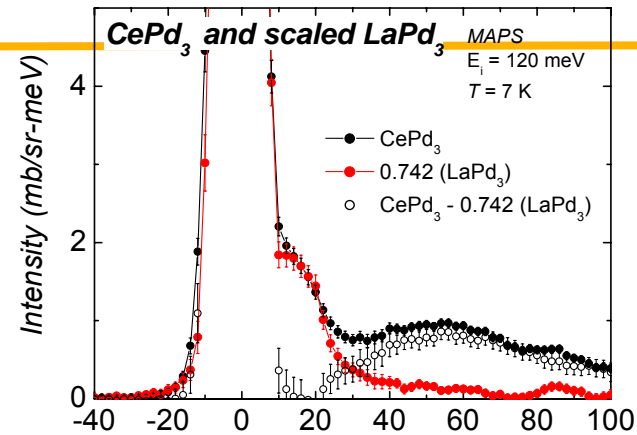
Slide 32



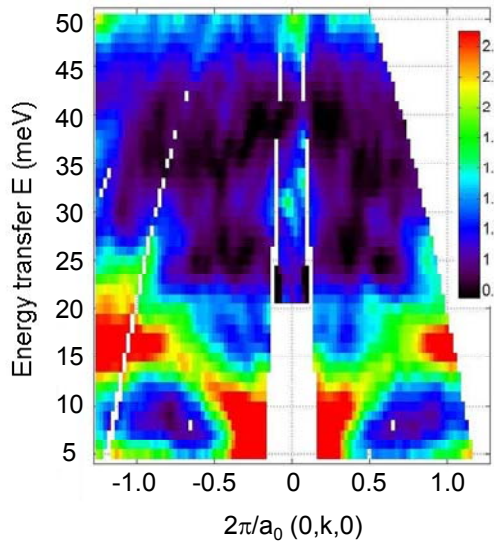
Non-magnetic
scattering

→

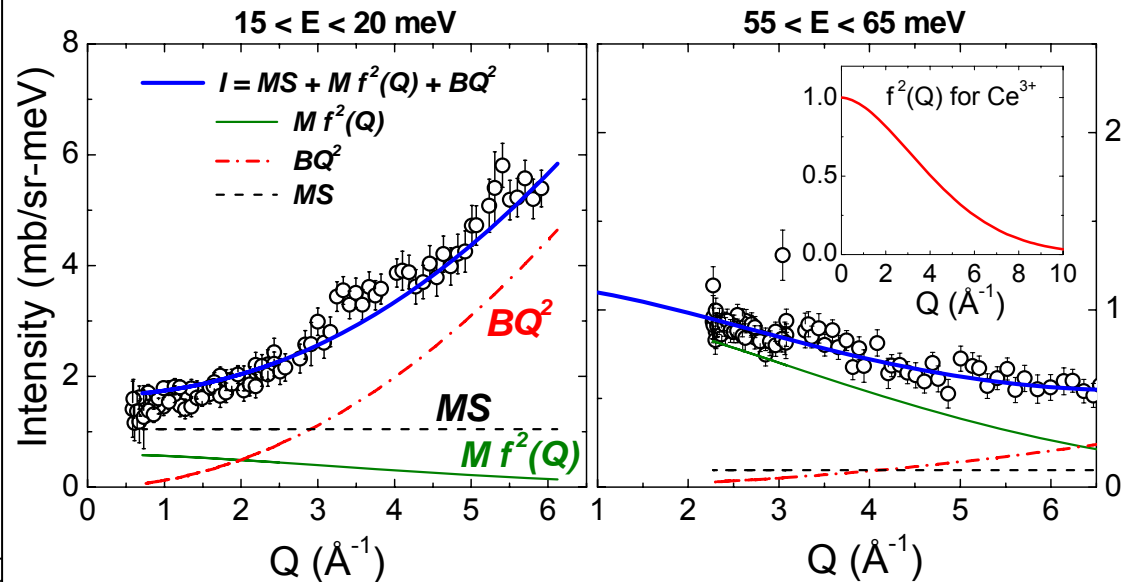
Represented as a
"scaled $LaPd_3$ "



Intensity color map E vs k

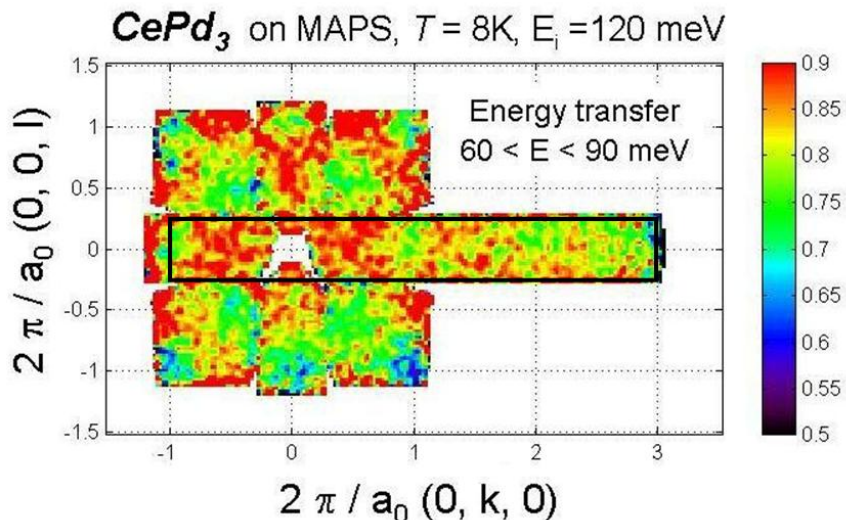


$CePd_3$ $E_i = 120$ meV, $T = 8$ K



Polycrystalline average (i)

- Integrate on a large portion of the reciprocal space



- Plot intensity I vs. Q for different ranges of energy transfer
- Analyze Intensity as composed by 3 contributions for the scattering:

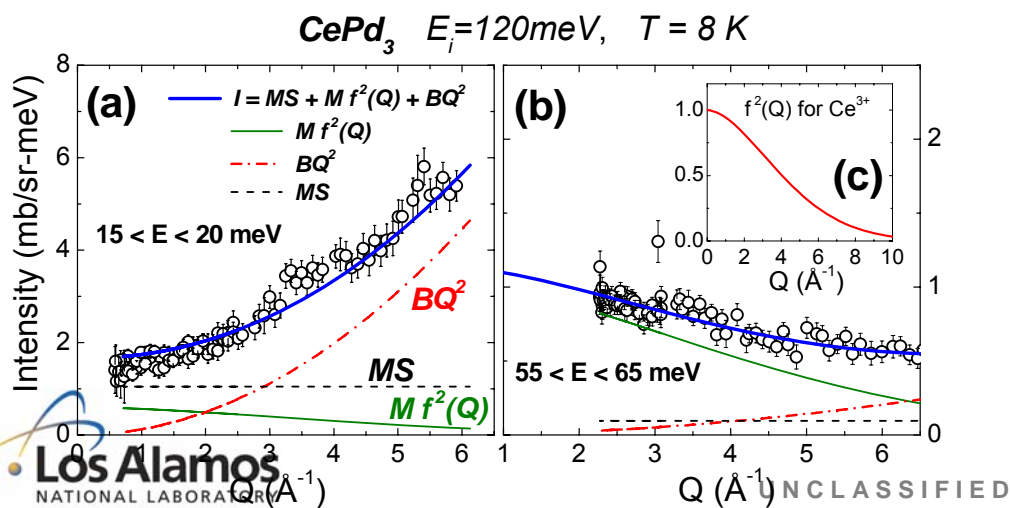
$$I = MS + BQ^2 + M f^2(Q)$$

Multiple scattering
Single phonon scattering
Magnetic scattering

$f^2(Q)$: magnetic form factor for Ce 4f orbital

Assumption:

MS and M are Q -independent

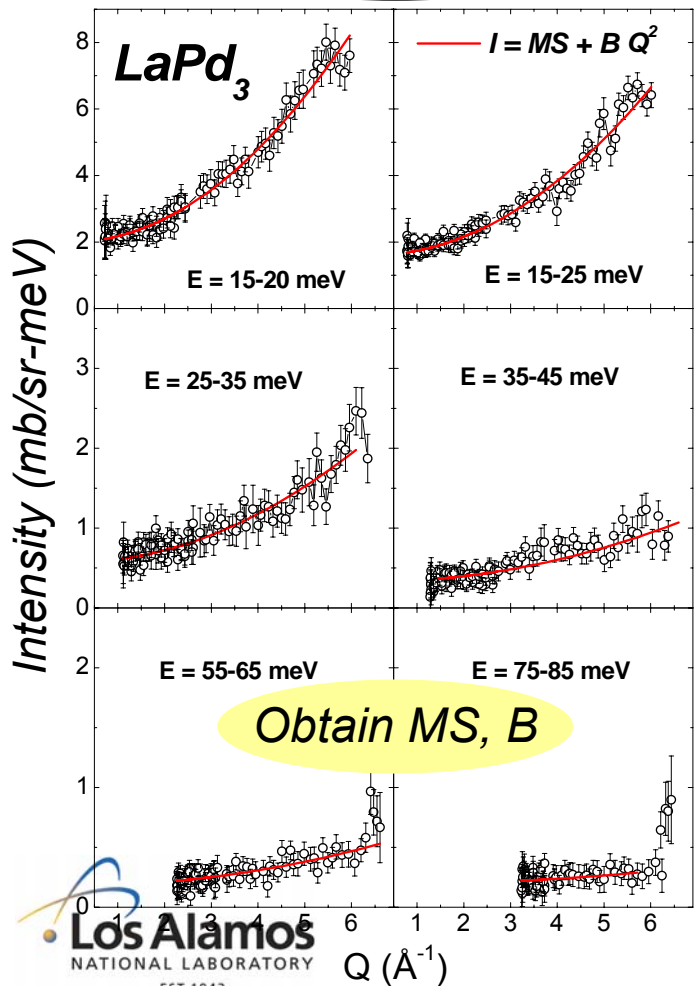


Polycrystalline average (ii)

Non-magnetic scattering from LaPd_3
 $MS+BQ^2$

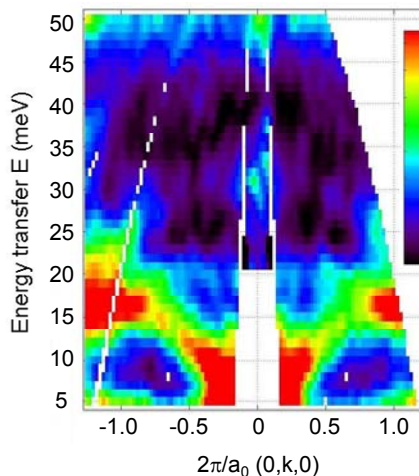
scaling $MS(\text{LaPd}_3)$,
 $B(\text{LaPd}_3)$

Magnetic scattering
 $I=MS + BQ^2 + M f^2(Q)$

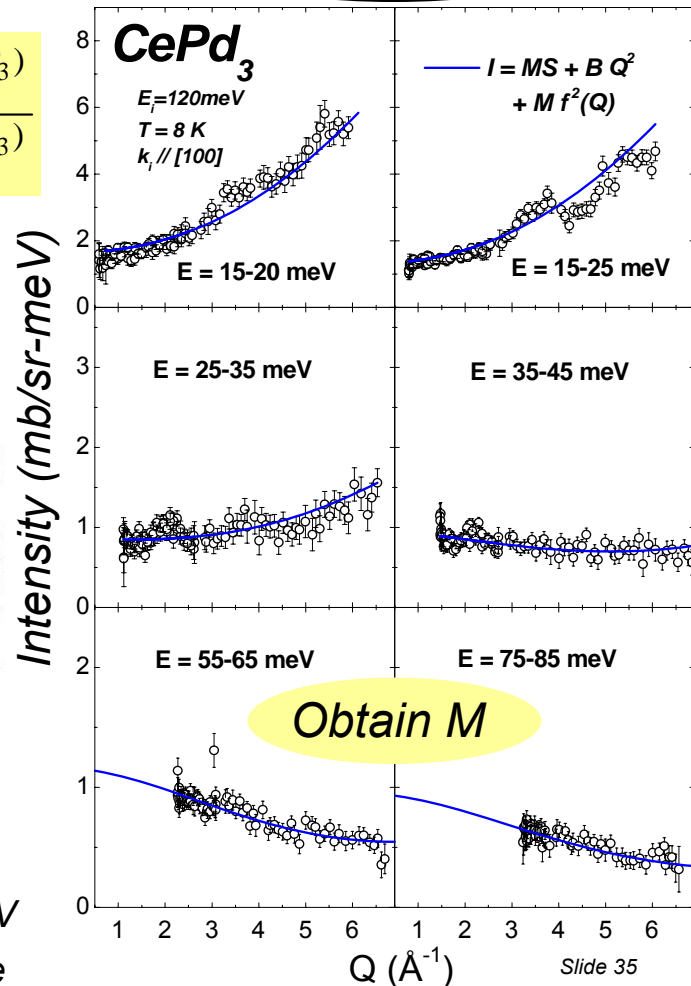


scale factor = $\frac{\sigma_{\text{coh}}(\text{CeP}_3)}{\sigma_{\text{coh}}(\text{LaP}_3)}$

ratio of **coherent scattering** cross sections



BQ^2 dominant < 30 meV
 $Mf^2(Q)$ dominant above
phonon cutoff



Polycrystalline average (iii)

$T = 8\text{ K}$: Inelastic Kondo-like magnetic scattering:

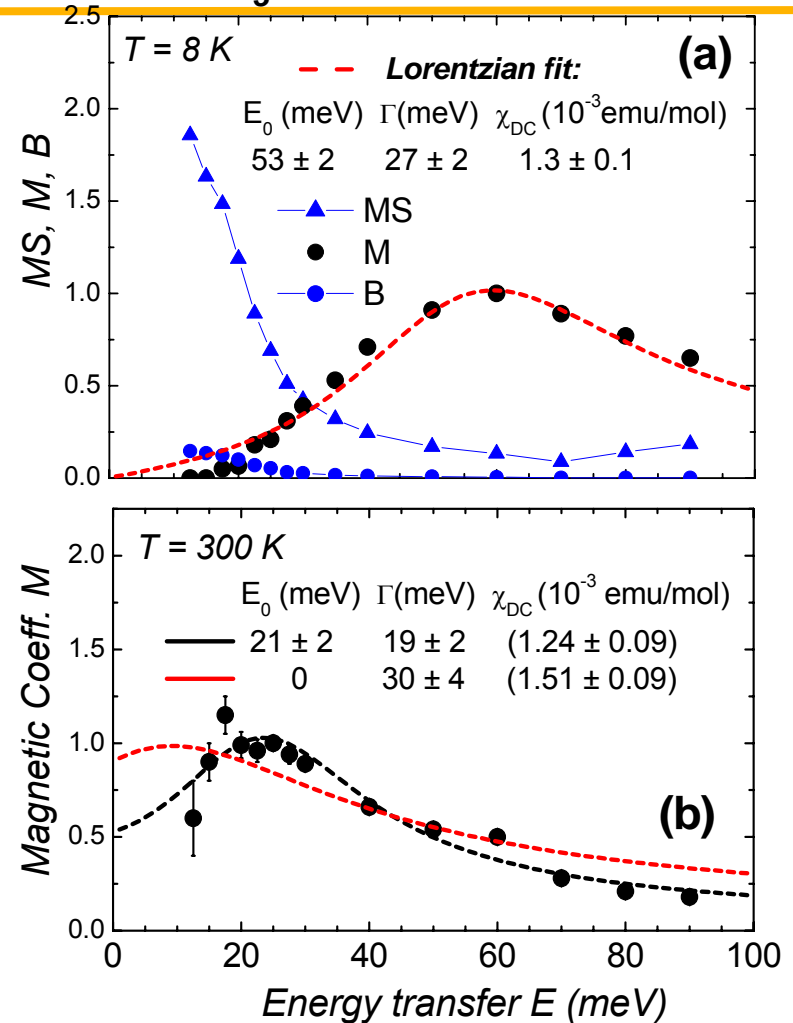
maximum between 50 and 60 meV, (same scale of $T_K \sim (500-600)\text{ K}$).

As temperature increases, it evolves towards a quasielastic Lorentzian

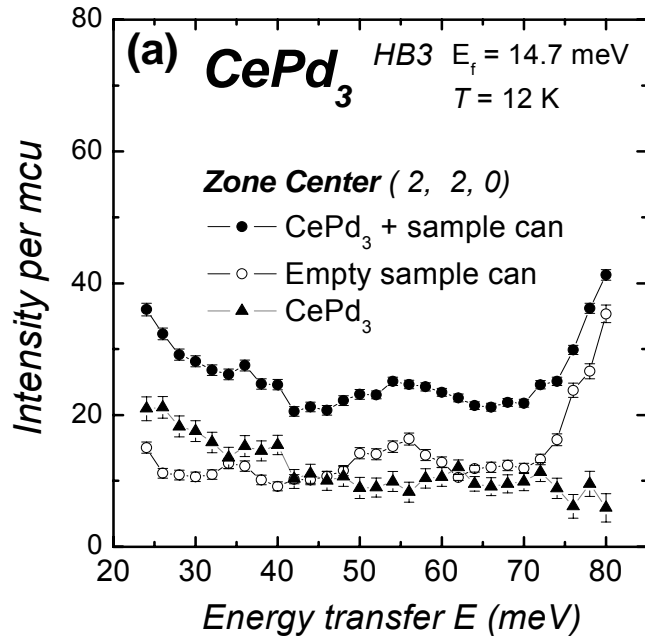
Scattering cross sections

Cross sections	σ_{coh} (barns)	σ_{inc} (barns)	$\sigma_{\text{total scatt}}$ (barns)	σ_{abs} (barns)	b_{coh} (fm)
La	8.53	1.13	9.66	8.94	8.24
Ce	2.94	0	2.94	0.63	4.84
Pd	4.39	0.093	4.48	6.9	5.91
LaPd ₃	21.70	1.409	23.10	29.64	25.97
CePd ₃	16.11	0.279	16.38	21.33	22.57
Ratio (CePd ₃ /LaPd ₃)	0.742	0.198	0.709	0.720	0.869

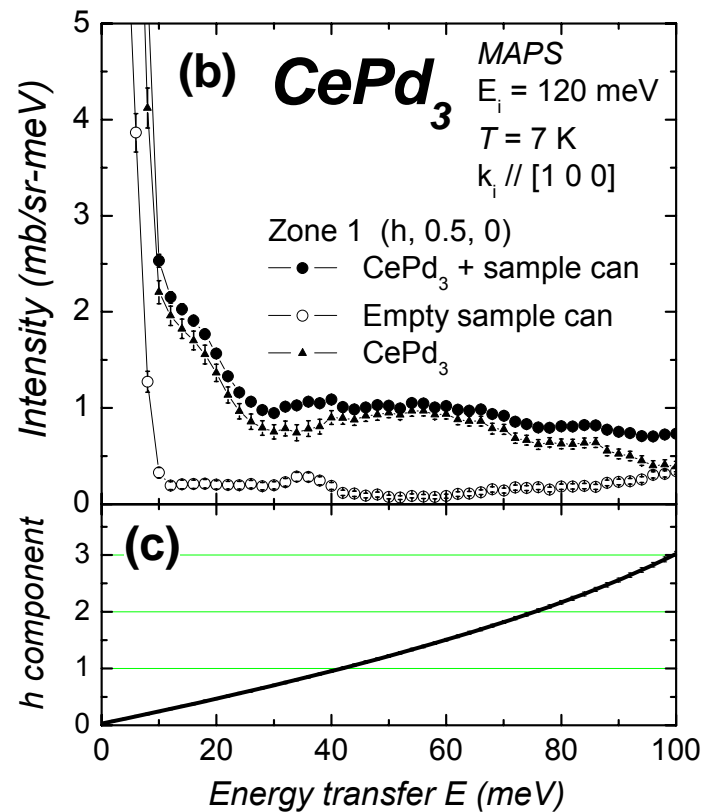
CePd₃ $E_i = 120\text{ meV}$



Comparison Triple-axis vs Time-of-flight spectrometers



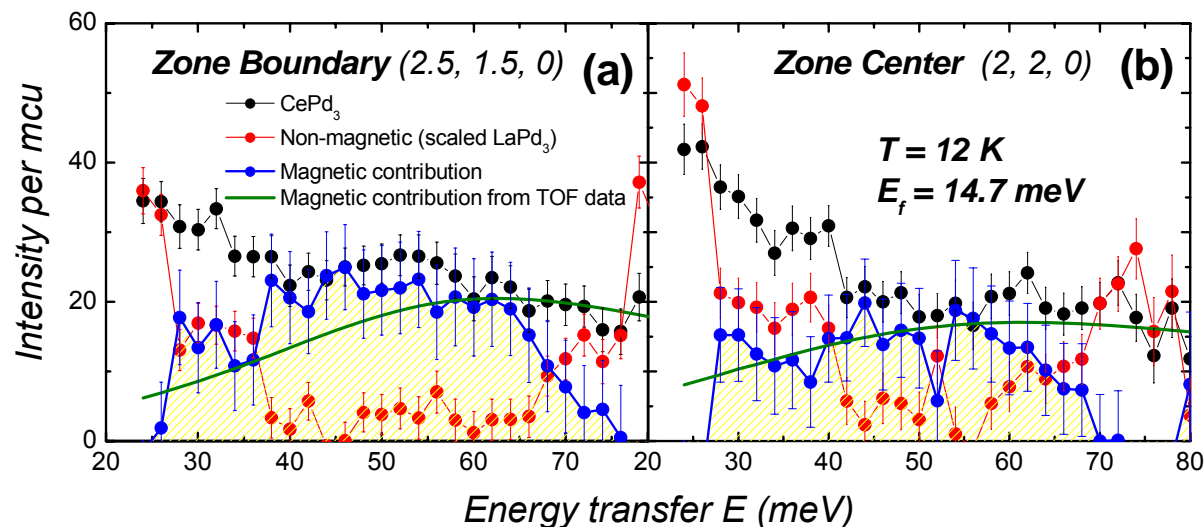
9 hs. of beam



12 hs. of beam

Measuring on Triple-axis spectrometer

HB3 Triple axis spectrometer $T = 12\text{ K}$, $E_f = 14.7\text{ meV}$



TAS has higher background, and lesser statistics:

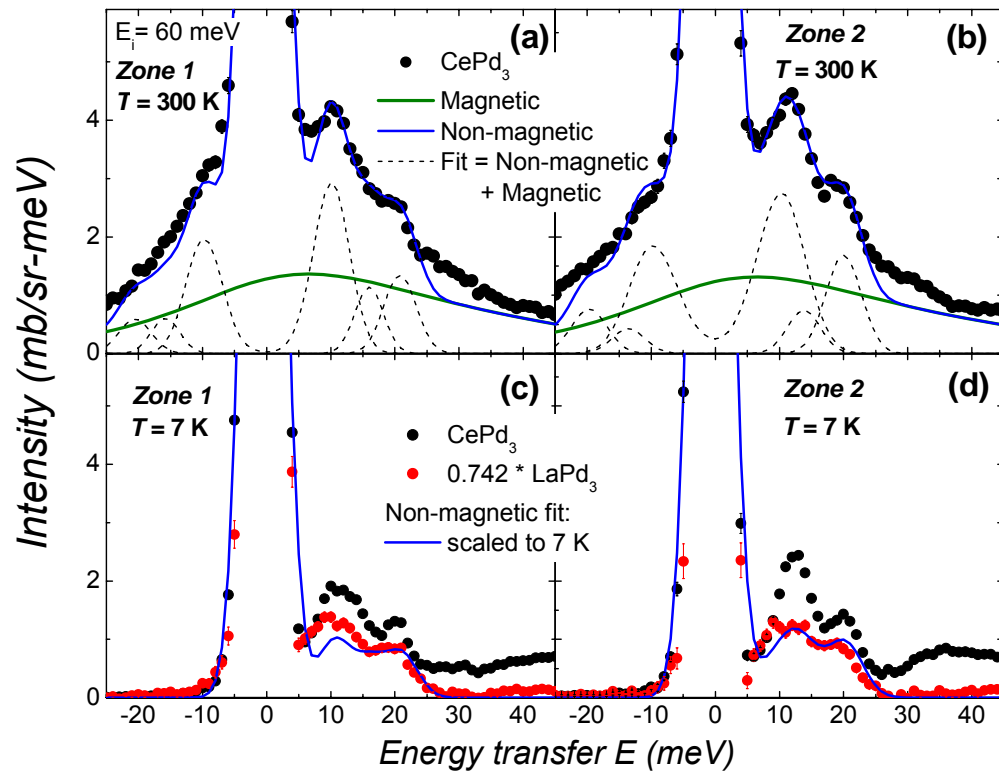
- Maxwell profile of the reactor ($\sim 70\text{ meV}$)
- Larger amount of aluminum “in the beam”

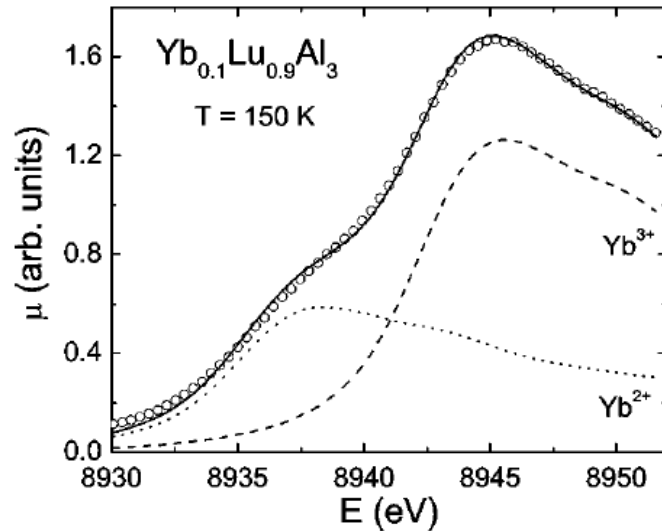
Constant Q - scans:

(a) Energy-scan at the Brillouin zone boundary, and (b) at the Brillouin zone center

The magnetic intensity from TOF measurements (green line) is also included for comparison.

Alternative Method to Obtain the Non-magnetic Scattering





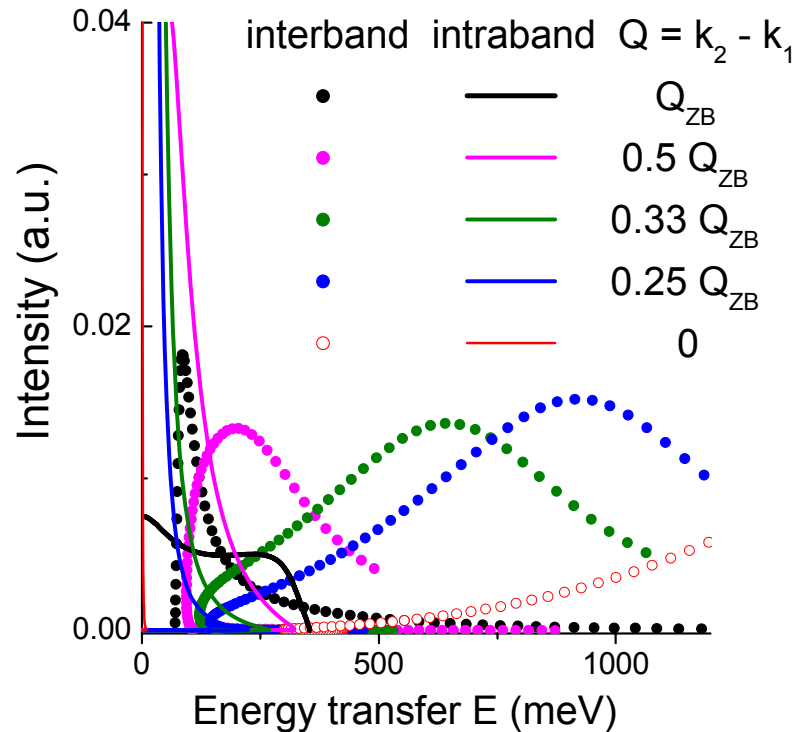
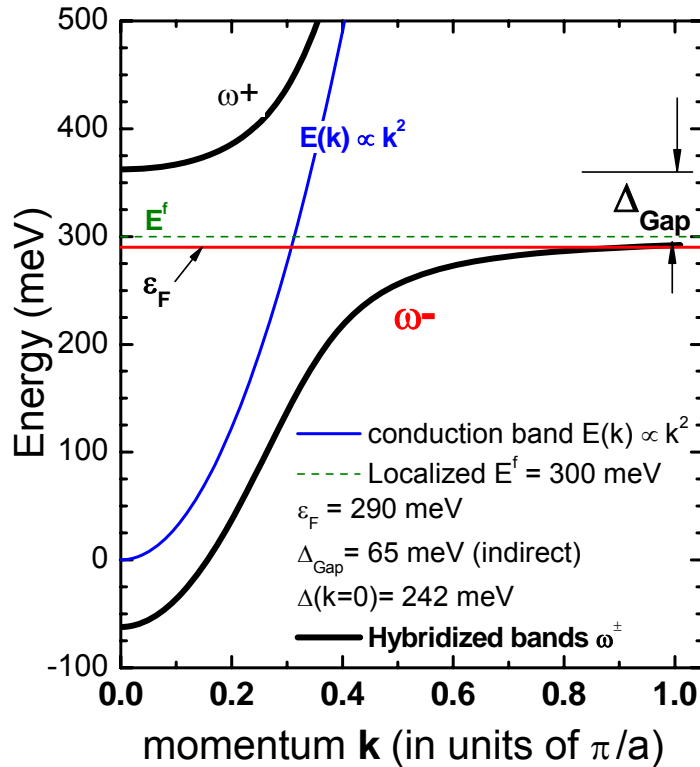
L_{III} X-ray absorption spectrum

*Spectra correspondent to
divalent and trivalent Yb
absorptions*

Bauer, *et al.*, Phys. Rev. B **69**,
125102 (2004)

Estimation for the spectrum of particle-hole excitations for a basic scheme of hybridized bands

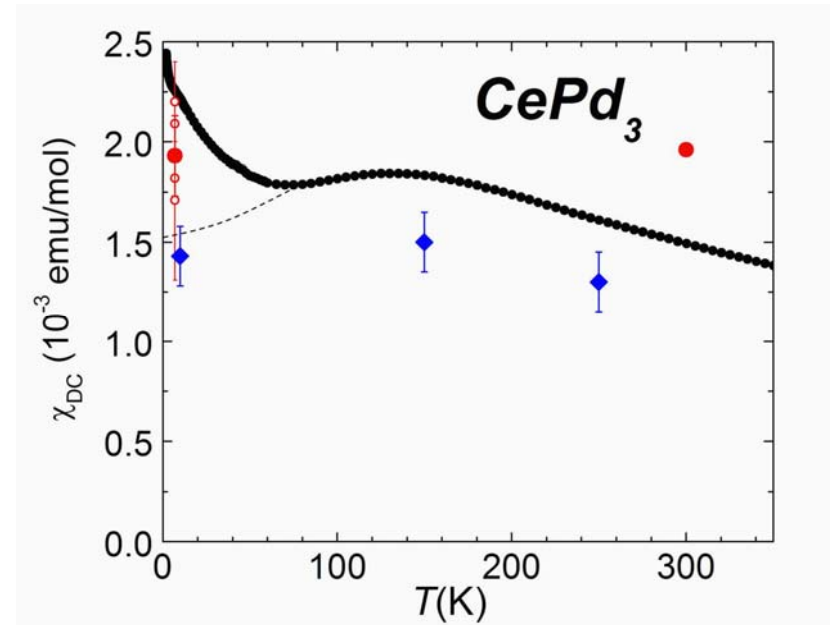
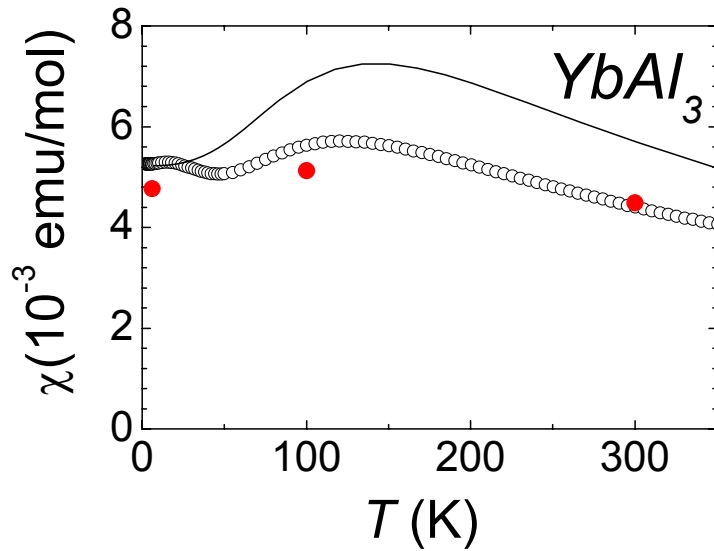
$$S(\vec{Q}, E) \propto \int dE' f(E') (1 - f(E')) D(E', E'+E; \vec{Q})$$



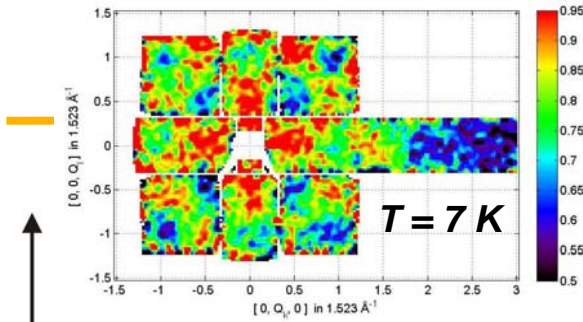
Spectra for intraband (lines) and interband (circles) excitations for momentum transfer in the range between 0 and $Q=Q_{\text{ZB}}$.

Magnetic Susceptibility

Bulk measurements and χ obtained from INS



Oscillation of Magnetic Intensity



Variations of order 20%

